ISSN 0016-8521, Geotectonics, 2023, Vol. 57, No. 4, pp. 446–459. © Pleiades Publishing, Inc., 2023.
Russian Text © The Author(s), 2023, published in Geotektonika, 2023, No. 4, pp. 103–117.

The Neotectonics and Geological Structure of the Sevan Intermountain Basin (Armenia): New Structural and Palaeontologic Data

E. A. Shalaeva[a], V. G. Trifonov[a, *], Ya. I. Trikhunkov[a], V. V. Titov[b], A. V. Avagyan[c], L. H. Sahakyan[c], A. N. Simakova[a], P. D. Frolov[a], S. A. Sokolov[a], M. A. Vasilyeva[a], D. M. Bachmanov[a], and G. M. Ovakymyan[c]

[a] *Geological Institute, Russian Academy of Sciences, Moscow, 119017 Russia*
[b] *South Scientific Center, Russian Academy of Sciences, Rostov-on-Don, 344006 Russia*
[c] *Institute of Geological Sciences, National Academy of Sciences of Armenia, Erevan, 0019 Armenia*
**e-mail: trifonov@ginras.ru*

Received August 8, 2022; revised November 2, 2022; repeatedly revised February 15, 2023; accepted February 16, 2023

Abstract—This article presents new data obtained as a result of field research in 2022 on the Sevan intermountain depression in Armenia. The emergence of the Sevan intermountain depression in the Miocene was associated with the development of the Sevan almond-shaped structure, which is bounded by the right-lateral Pambak–Sevan–Syunik fault zone in the northeast, the Garni zone in the southwest, and the Arpa–Zangezur zone in the south. Within the Sevan almond-shaped structure, the strike-slip structures of Lesser Sevan (the western part of Lake Sevan) and the Gavar almond-shaped structure, the Gavar horst, a number of faults, as well as extension zones were formed, including the southern part of Greater Sevan (the eastern part of Lake Sevan) and the axial zone of the Geghama Range. The development of the Sevan intermountain depression continued in the Pliocene under the influence of the uplift of the Lesser Caucasus and the Armenian Highlands. We have summarized the available data on the geological structure and geodynamics of the Sevan intermountain depression; we present the obtained data on the stratigraphy of the Pliocene–Quaternary deposits and their position, and show that during the Akchagyl transgression at the Pliocene–Pleistocene boundary, marine sedimentary accumulations did not occur in the Sevan intermountain depression.

Keywords: neotectonics, Armenian Highlands, intermountain depression, active faults, Akchagyl transgression, lacustrine sediments, Pleistocene fauna

DOI: 10.1134/S0016852123020073

INTRODUCTION

The Sevan intermountain depression is located on the Armenian Highlands. The basin extends for 85 km in length and 43 km in width, and is one of the largest structures in the highlands (Fig. 1). The depression is divided into two basins, that is, the Lesser Sevan and Greater Sevan. The depth of the Lesser Sevan reaches 80 m, the depth of Greater Sevan ranges from 19 m to 30 m. At that time, the mountain structure of the Lesser Caucasus and the Armenian Highlands was rising, in which regional fault zones were formed, and active volcanism was also developing, which determined the features of the tectonics and geological structure of the Sevan intermountain depression.

The purpose of this article was to analyze the structure, reconstruct the history of the Late Cenozoic development, identify the nature and tectonic conditions for the formation of the Sevan intermountain basin on the basis of the available materials and those obtained by us on the tectonics and stratigraphy of the basin, including new data on magnetostratigraphy, isotope dating, spore-pollen analysis, and a unique find of the remains of an extinct species of deer, *Arvernoceros*.

THE GEOLOGICAL OUTLINE

The northeastern side of the Sevan intermountain depression is represented by the Sevan–Akera ophiolite zone marking the Upper Cretaceous Tethys suture. The ultramafic and basic rocks of the ophiolite nappes occur as large undeformed plates or form zones of serpentinite melange, in places underlain by olistostromal strata [7, 10, 21, 27, 31].

The ophiolite complex is overlain by the Campanian terrigenous-detrital sequence, composed mainly of red-purple and green pebbles, which are erosion products of ophiolites stretching along the northeast banks of the Greater Sevan. Above the terrigenous-

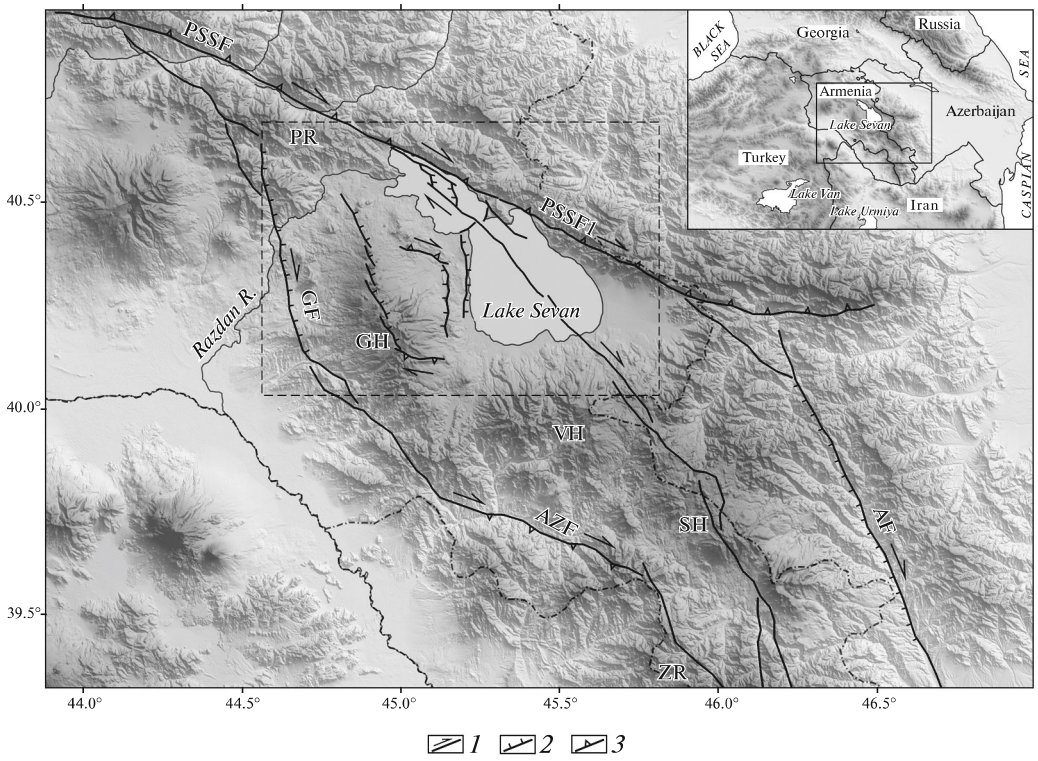

Fig. 1. The Sevan almond-shaped structure (modified after [23]). Inset: position of the study region. Pambak–Sevan–Syunik fault zone: PSSR, northern branch; PSSR-1, southeastern branch. Faults: GR, Garni; AR, Akerinsky; AZR, Arpa-Zangezur. Volcanic Highlands: GN, Geghama; VN, Vardenis; SN, Syunik. Ridges: PKh, Pambakskii; ZR, Zangezur. (*1*)–(*3*) faults: (*1*) strike-slip; (*2*) normal; (*3*) thrust and reverse.

clastic stratum, there are Campanian–Maastrichtian limestones, flyschoid strata, marls, and nummulite limestones of the Eocene, as well as Eocene volcanic rocks of basalt, basaltic andesite, andesite, and trachyandesite composition [6, 7, 10, 29].

This complex of rocks composes the modern structures of the Aregun and East Sevan ranges, which were formed in Miocene–Quaternary time as part of the mountain structure of the Lesser Caucasus. We assume that the ophiolites of the Sevan–Akerin zone underlie the Sevan intermountain depression. The remnants of these covers are exposed to the southwest of Lake Sevan in the valley of the Vedi River. The obduction time of the ophiolites is the Coniacian-Santonian interval [7, 10, 31].

The southern side of the Sevan intermountain depression is formed by the northern slopes of the Vardenis volcanic highlands. In the water divide part on east highlands Cretaceous–Paleocene basalts, limestones, sandstones, siltstones, and mudstones are locally exposed. Above, predominantly volcanic strata lie, interbedded with volcanic-sedimentary rocks with a thickness of several kilometers [11, 12]:

— basaltic andesites, andesites and rhyodacites (Middle Eocene);

— andesites, tuff breccias and tuff sandstones of andesitic composition (Upper Eocene);

— dacites and rhyolites (Upper Eocene–Oligocene);

— rhyolites and rhyodacites (Lower Miocene);

— rhyolites and rhyodacites with andesites (Lower–Middle Pliocene);

— dolerite basalts (Upper Pliocene);

— basalts, basaltic andesites and andesites (Quaternary);

— andesites (Holocene) expressed as the youngest streams, located in the north of the Vardenis Highlands.

The western wall is formed by lava flows of the Geghama Highlands, which formed in the Upper Miocene–Quaternary. The oldest known rocks are 5.7–4.6 Ma and are predominantly trachyandesites in the western part of the highlands. Volcanic activity of the end of the Pliocene–beginning of the Quaternary period (Akchagyl time) manifested itself, apparently, on a limited scale, in the north of the highlands, in the valley of the Razdan River, where the plateau basalts of the subalkaline series formed ~2.5 Ma ago. Starting from ~0.7 Ma, four phases of volcanic activity were distinguished in the history of the Geghama Highlands with a peak of activity ~0.2 Ma ago, when most

of the monogenic cones (more than 100) formed in the axial part of the Geghama Highlands and the volcanoes of the Eratumber group and west coast of Lake Sevan. Most of the products of volcanic activity are represented by trachyandesites and basaltic trachyandesites [2].

The Late Cenozoic Structure of the Sevan Basin and Its Surroundings

In the Sevan region, which includes the southeastern spurs of the Pambak ridge, the Sevan depression, the Geghama, Vardenis, and Syunik volcanic highlands, and the northern part of the Zangezur ridge, a peculiar combination of Late Cenozoic structural elements, called the Sevan almond-shaped structure, has been exposed [23, 25] (see Fig. 1).

The almond-shaped structure is a strike-slip formation, which, unlike pull-apart structures, is large and develops not between segments of the same strike-slip zone, but between different strike-slip zones, in this case, dextral strike-slips, limiting the almond-shaped structure from the northeast (Pambak–Sevan–Syunik zone) and southwest (Garni and Arpa–Zangezur zones). According to GPS observations, the development of the Sevan almond-shaped structure as a uniform structure occurs under conditions of transverse compression with its axis oriented to the north-northeast and tension with the axis oriented to the west–east, as is characteristic of the whole territory of Armenia [15].

The Sevan intermountain depression is located in the northern part of the Sevan almond-shaped structure. From the northwest to the southeast, the depression is formed by the Tsovagyukh graben, which continues to the east with the lake depression of Lesser Sevan, and the lake depression of the Greater Sevan, which continues to the southeast into the coastal Masrik lowland. The Lesser and Greater Sevan depressions are separated by a tectonic bridge, which during periods of complete drainage of the Greater Sevan in the Pleistocene was dissected by an antecedent fragment of the Razdan River valley.

The Pambak—Sevan–Syunik fault system, which limits the almond-shaped structure from the northeast, is the largest Quaternary fault zone in Armenia. Dextral slips dominate along it, whose rate varies from 1.2 ± 0.9 to 2.4 ± 0.6 mm/yr [20, 24]. The reverse fault component of displacements is variable and is subordinate: the northern flank is uplifted [23, 25] (see Fig. 1). Within the boundaries of the Lesser Sevan, the Pambak–Sevan–Syunik fault zone bifurcates into northern and southern branches. The northern branch extends further to the east, where the southeast-trending Akerinsky Fault separates from it (presumably by dextral strike-slip) and to the east the northern branch fades. The southern branch follows the southeast along the bottom of the Greater Sevan and further along the Syunik highlands. The dextral slip rate along the southern branch reaches 4–5 mm/yr, multiply exceeding the fault component of displacements [24]. The southern branch and the Akerinsky fault are bounded in the south by the Araks zone of sinistral strike-slips [11].

In the west, the almond-shaped structure is limited by the Garni with dextral slip with a subordinate vertical component of movement. The shear rate has been estimated at 2 mm/year [32]. The element of the southern boundary of the almond-shaped structure is the Arpa–Zangezur fault zone [23]. It is formed by a number of relatively short faults, branching in places and having an echelon arrangement relative to each other. Along the faults, signs of dextral and vertical strike-slip faults were found and the southern flank is more often uplifted.

Thus, the Sevan almond-shaped structure is bounded by faults with a dominant dextral strike-slip component. At the same time, in the WNW–ESE-trending faults, it is combined with the upthrow fault component, and in the NNW–SSE-trending faults, it is combined with the downthrow fault component.

Inside the almond-shaped structure, local faults and their combinations are identified, forming structural forms of the second order. Movements on them provide an extension rate of 2.4 ± 0.9 mm/yr south of the Sevan depression and 1.5 ± 0.8 mm/year in the northern part of the Geghama highlands [20]. Within the limits of Lesser Sevan, between the two branches of the Pambak–Sevan–Syunik fault zone, a pull-apart structure arose. Its descent is caused by the greater depth of Lesser Sevan compared to Greater Sevan.

We have refined the structure of structural forms of the second order in the southwestern framing of the Sevan depression (Fig. 2).

The Geghama almond-shaped structure of the second order was found in the Geghama Highlands [11, 15]. From the north and east, it is limited by the Gavarageti Fault Zone (GRZ-1). The most expressed element of the zone is the Kamo fault [11]. The west–northwestern segment of the Kamo fault is characterized by dextral reverse-strike-slip displacements; the meridional segment by strike-slip displacements with a lowering of the west wing. The maximum revealed amplitude of the Late Quaternary dextral strike-slip along the meridional segment is ~260 m; the vertical amplitude varies from 70 to 170 m and possibly reaches 250 m [15].

The southwestern limit of the Geghama almond-shaped structure has a meridional strike in the north and southeast in the more southern segments. The eastern flank of the fault is lower. In the meridional segment, the vertical displacement is normal and in the southeastern segment, the displacement is reverse.

This limitation is formed by the central chain of Late Pleistocene volcanic cones of the Geghama

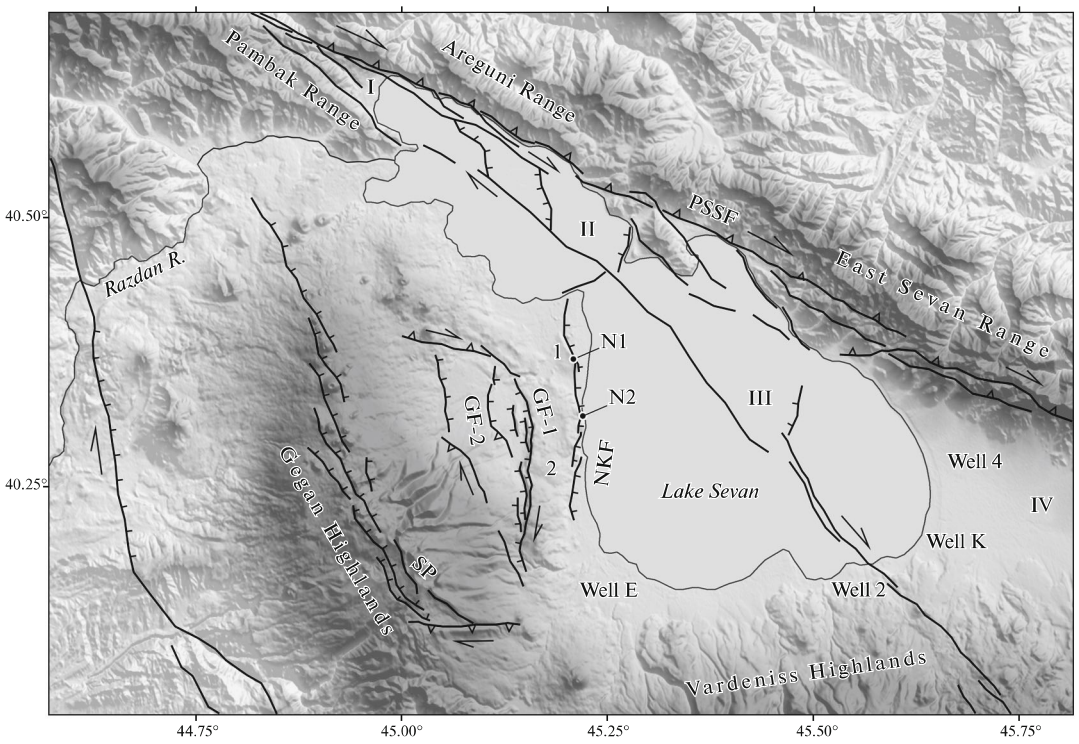

Fig. 2. The Late Cenozoic structure of the Sevan intermountain depression and its southwestern framing. Designated (Roman numerals): (I) Tsovagyukh graben; (II) Lesser Sevan (pull apart); (III) trough of the Greater Sevan; (IV) Masrik depression. Designated (Arabic numerals): (1) Noratus fault; (2) Gavar horst. Fault zones: PSSR, Pambak-Sevan-Syunik; NKF, Noratus-Kanagekhskaya; SP, Spitaksarskaya. Branches of the Gavar fault: GRZ-1, northeast; GRZ-2, southwestern. Pliocene–Quaternary outcrops: H1, Noratus-1; H2, Noratus-2. Wells: well 2, Norakert; well 4, Nasosnaya; well E, Yeranos; well K, Karchaghbyur-1.

Highlands extending to the north-northwest, which in the south passes into a series of parallel faults of the Spitaksar zone with lower eastern wings. Separate normal faults are expressed in relief as ledges with an amplitude of up to 15 m. Further south, the strike of the Spitaksar zone changes to the southeast. Faults acquire a slope up to ∟70° to the southwest towards the raised wing, i.e., become reverse faults. The reverse fault component of the displacement is combined with the superior dextral strike-slip component. Along one of the faults in the zone, the strike-slip amplitude is 30–50 m with uplift by 10–15 m. Along the other fault, the moraine is upthrown by 2–3 m where shallow streams cut into it are sheared by 16–20 m [11].

Part of the almond-shaped structure between the branches of the Gavarageti fault forms a depression. Numerous small faults are observed within its limits (Fig. 3b).

To the east of the Geghama almond-shaped structure, the meridional Noratus–Konagekh fault extends (see Fig. 3a). Between this fault and the meridional segment of the Kamo fault of the Gavaraget fault zone is the Gavar horst.

THE STRATIGRAPHY OF THE NEOGENE–QUATERNARY SEDIMENTARY DEPOSITS

In our study, we used the Eastern Paratethys stratigraphic scale, whose regional stages have the following time intervals:

— 13.7–7.6 Ma (Sarmatian);
— 7.6–7.0 Ma (Meotis);
— 7.0–5.3 Ma (Pontian);
— 5.3–3.2 Ma (Cimmerian);
— 3.2–2.1 (1.8) Ma (Akchagyl);
— 2.1 (1.8) –0.8 Ma (Apsheronian);
— 0.8–0.01 Ma (Baku and Khazar horizons).

Neogene sedimentary deposits older than the middle-upper Sarmatian in the Sevan depression are unknown. Deposits of the Sarmatian regional stage accumulated in the conditions of the Ponto-Caspian Bay and are represented by clays, weakly lithified siltstones, and sandstones containing the leading forms of the Sarmatian malacofauna. Deposits come to the surface in the middle reaches of the Razdan river and well 2 (Norakert) and well 4 (Pumping) drilled in the coastal zone of Lake Sevan, as well as the Karchaghbyur-1 well in the depth interval 305–410 m and the Yeranos-1 well drilled to depths of 1170 m [9, 12] (Fig. 4).

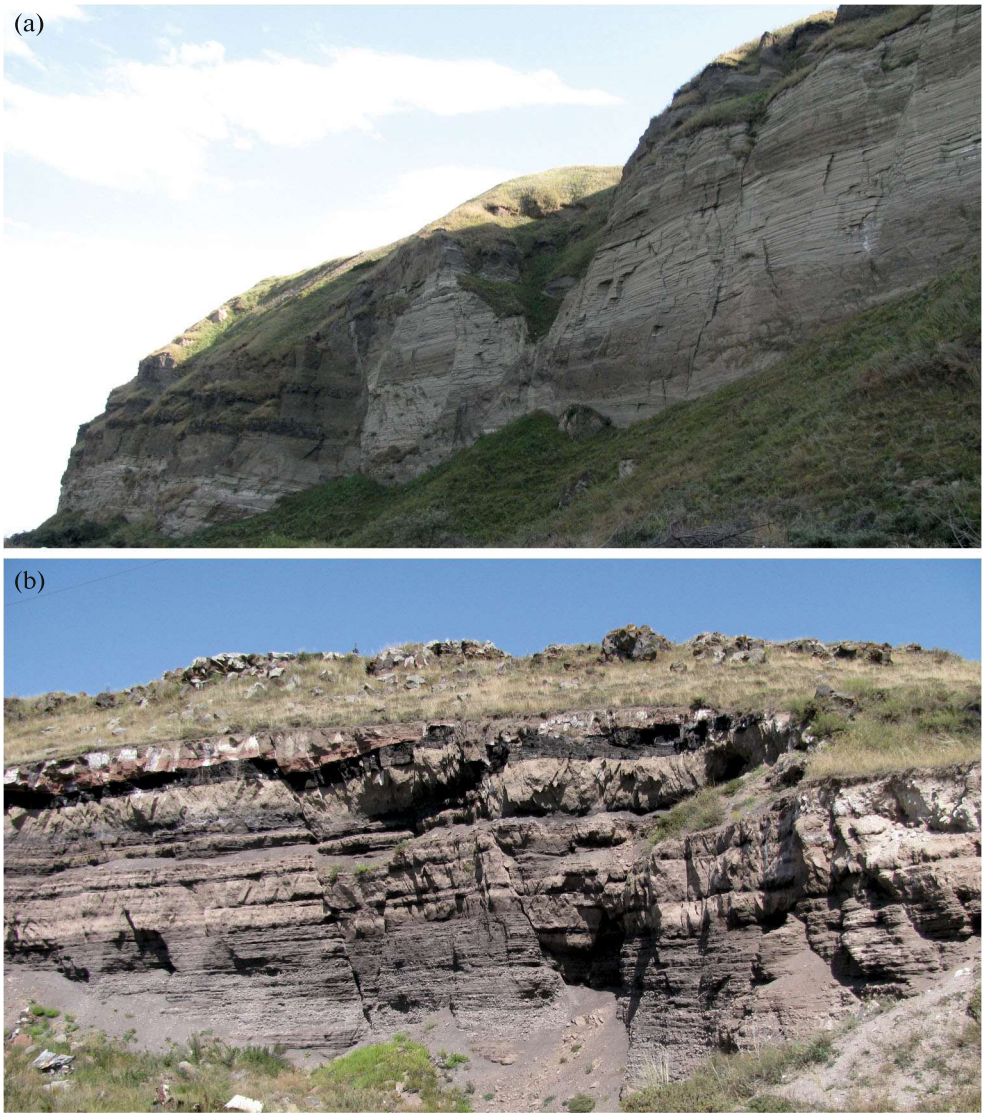

Fig. 3. Photos of the Noratus-1 fault. (a) Noratus-1 outcrop (Noratus fault); (b) shallow faults within the activity zone of the Gavarageti fault.

The overlying deposits accumulated in conditions isolated from the Ponto-Caspian: the Meotic deposits were still in the brackish water basin, while the younger ones were accumulated in a freshwater lake reservoir or had an alluvial-proluvial genesis.

The only known area of outcropping of sedimentary Upper Miocene–Quaternary sediments is a strip of outcrops along the western coast of Greater Sevan, united by the common name of the Noratussky section (or Sarykainskaya stratum) with a total thickness of ~300 m [8, 9].

E.E. Milanovsky [8] identified eight formations in this sequence.

Yu.V. Sayadyan [9] specified the formation time intervals and attempted to correlate the coastal deposits with the data from well 2 (Norakert) and well 4 (Nasosnaya) (Fig. 4).

The lithological similarity of deposits of different formations, the fragmentation of their exposure to the day surface and the almost complete absence of faunal finds make it difficult to describe the sequence.

Formations I and II of the Noratus section build up the Artsvakar anticline (~40°19′57.47″ N, 45°10′43.15″ E), which is not currently exposed [8, 9]. The carbonate-terrigenous marine deposits of formation I are presumably assigned to the Sarmatian. The tuffaceous-terrigenous formation II, assigned to the Maeotis and Pontus, is missing in sections of wells 2 and 4.

Formation III with angular unconformity and erosion overlies the underlying formations and is composed of lacustrine diatomites and sand–gravel–pebble deposits. To the south, they are replaced by rhyolitic tuffs, which were compared with tuffs of the corresponding intervals of borehole sections 2 (622–501 m) and 4 (560–396 m) [9]; the isotope age of 4.8 Ma was deter-

mined for them [3], which allowed their attribution to formation III to the Lower Pliocene (Cimmerian).

At the base of formation IV, lacustrine-alluvial deposits with dacitic lava flows were attributed to the Upper Pliocene [8] (taking into account the modern boundary between the Pliocene and Pleistocene, to Akchagyl).

Andesite basalts were identified as formation V, which were called Manychar lavas [8].

Formation VI, the Noratus proper, exposed in the ledge of the Norratus fault, was considered as Pleistocene [8] or Lower Pleistocene (Apsheron) [9], and the Uch-Tapolyarsky lava cover and modern lacustrine-alluvial deposits were attributed to formations VII and VIII.

In order to analyze the indicated stratigraphic scheme and clarify the history of the formation of the Sevan intermountain depression, we studied the Noratus-1 and Noratus-2 sections on the western coast of Greater Sevan. The Noratus-1 section is located directly in the wall of the Noratus fault scarp (see Fig. 3a). The Noratus-2 section is located to the south in the lowered limb of the Noratus–Konagekh fault zone (see Fig. 2).

The Noratus-1 and Noratus-2 Sections on the Western Coast of Greater Sevan

Noratus-1. This outcrop (40°22′07.78″ N, 45°12′22.03″ E, $h = 2000$ m) is represented by the following sequence of layers from top to bottom [16] (Fig. 5):

— layer 1, brown pebbles and tuff breccias, unstratified, inclusions of unrounded fragments of andesites and dacites, in the upper part there are two layers of black pumice 0.5–1-m thick, layer thickness up to 12 m;

— layer 2, silt (gray-beige, horizontally bedded, interlayers of diatomites, fine-grained sandstones, less often gravel and small pebbles (washed slag), oolitic textures in silts), layer thickness is 11 m;

— layer 3, tuff breccia (gray-beige, consisting of fragments of mainly pumice and gravel-sized slags with interlayers of poorly sorted sandstone, single inclusions of poorly rounded pebbles), the thickness of the layer is 7 m;

— layer 4, gravel (dark gray, unlayered), in the roof there is a lenticular layer (up to 0.5-m thick of fine-grained thin-layered light sand with scattered unrounded fragments of volcanic rocks), the thickness of the layers is 2 m;

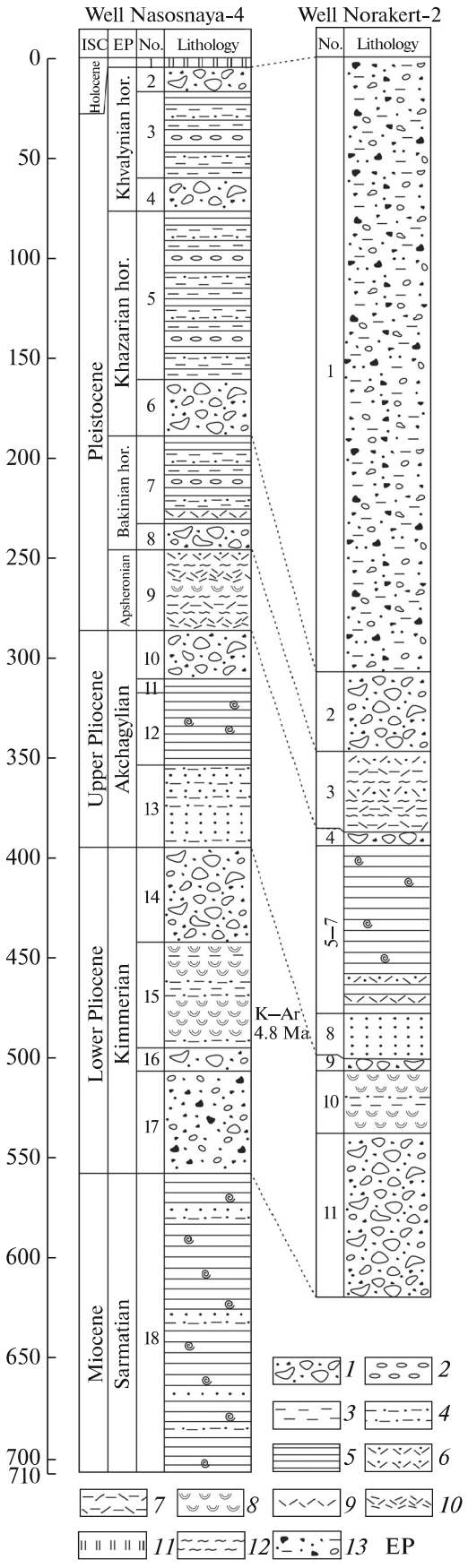

Fig. 4. The geological columns for wells No. 2 (Norakert) and No. 4 (Nasosnaya), the southern coast of Greater Sevan (according to [9] with changes and additions). Designated: EP, Eastern Paratethys scale. (*1*) Boulders, pebbles, gravel; (*2*) flat, rolled pebbles; (*3*) loams; (*4*) sandy loam; (*5*) clay; (*6*) tuff sandstones; (*7*) tuff aleurites; (*8*) tuffs, ignimbrites; (*9*) ashes; (*10*) rhyolites, pumice; (*11*) peat; (*12*) diatomites; (*13*) deluvium.

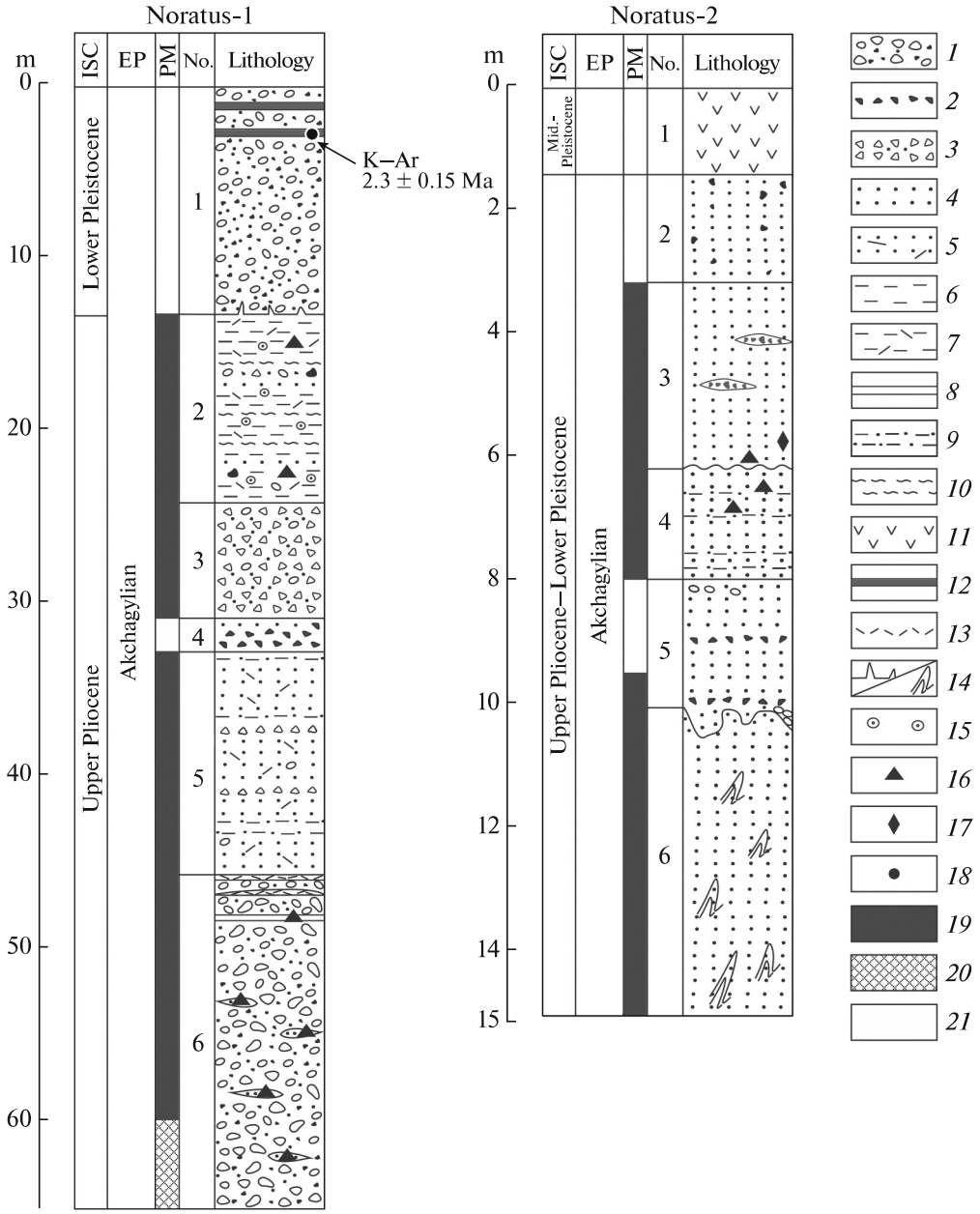

Fig. 5. Geological columns of outcrops Noratus-1, Noratus-2. Position N1, N2, see Fig. 2. (*1*) Pebbles, gravel; (*2*) gravel; (*3*) tuff breccia; (*4*) sandstone; (*5*) tuff sandstone; (*6*) silt; (*7*) tuff aleurite; (*8*) clay; (*9*) siltstone; (*10*) diatomite; (*11*) andesite; (*12*) pumice; (*13*) volcanic ash; (*14*) seismites; (*15*) ooliths; (*16*) spore-pollen samples; (*17*) faunal find *Arvernoceros* sp.; (*18*) sample for K–Ar dating; (*19–20*) residual magnetization: (*19*) straight, (*20*) reverse, (*21*) unknown.

— layer 5, sandstone (gray, weakly lithified, thinly bedded, horizontally bedded), thin interlayers of rewashed pumice and gravel slag dimensions, silts, single inclusions of pebbles, the thickness of the layers is 10–12 m;

— layer 6, boulder-pebble horizon with sand-gravel filler, mainly from effusives of andesite, basaltic andesite and basalt composition, less often dacite or pebbles from tuffs, sorting weak, the texture is mostly non-layered, locally cross-layered, layering is inclined or filling of transverse gullies, as well as inclusions of small lenses of sand, silt or rewashed ash; is 18–20 m.

For layers 2–6 95 samples were taken for paleomagnetic research. The lower 12 samples (lower ~5 m of layer 6) showed reverse magnetization, the rest showed direct magnetization.

Two pumice samples were taken from layer 1 for K–Ar dating.

K–Ar dating was performed at the Laboratory of Isotope Geochemistry and Geochronology IGEM RAS

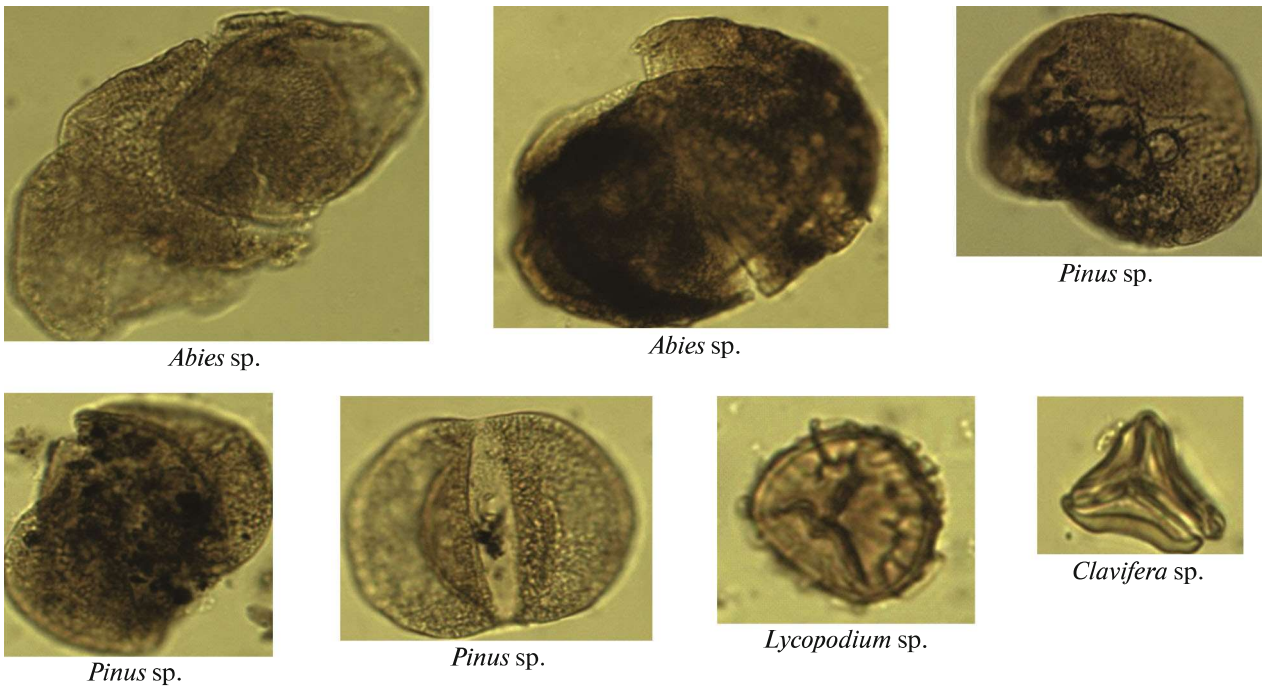

Fig. 6. Pollen grains from the Noratus-1 outcrop.

(Moscow, Russia). The age of the sample from the upper layer is 2.30 ± 0.15 Ma, and that of the lower layer is 1.8 ± 0.2 Ma. A sample from the lower layer showed a high content of atmospheric ^{40}Ar, which was therefore excluded from consideration.

In layers 4–6, samples were taken for spore-pollen analysis (Fig. 6). Single pollen grains of the Neogene flora were found, *Abies* sp., *Pinus* sp., *Picea* sp., *Clavifera* sp., and *Lycopodium* sp., no malacofauna.

Noratus-2. This outcrop (40°19′52.08″ N, 45°12′39.58″ E, h = 1930 m) is represented by the following sequence of layers (top-down) (see Figs. 5, 7):

— layer 1', andesites (Manychar lavas), layer thickness is 1.5 m;

— layer 2', unstratified yellow sandstone, weakly lithified, gravel inclusions, layer thickness is 2.2 m;

— layer 3', cross-bedded yellow sandstone, weakly lithified, gravel lenses (effusives, pumice, slag), ripple marks, four layers of dense sandstone, layer thickness is 3 m;

— layer 4', alternating thin interlayers of pink siltstones and dark gray fine-grained sandstones, in the upper part, rewashed gravel pumice dimensions, the thickness of the layer is 1.5–1.8 m;

— layer 5', horizontally layered sandstone (dark gray) with gravel interlayer, layer thickness is 1.7 m;

— layer 6', fine-grained sandstone (dark gray) is massive, intense intralayer deformations are seismites, contact with the overlying layer is erosive.

Twenty-one samples were selected for paleomagnetic studies, all samples showed normal magnetization.

Samples taken for spore-pollen analysis showed the complete absence of pollen grains, malacofauna is also absent.

Deer bone remains were found in layer 3'. The fragment of the right discarded horn with a broken rod and supraorbital process (collection of the National Academy of Sciences of the Republic of Armenia, IGN no. 10219/HSH 4118) belonged to a medium-sized deer (Table 1). The horn is characterized by a rod that is round in cross section and devoid of other branches at a distance of at least 14 cm from the supraorbital process (Fig. 8). The first supraorbital process is round in cross section. It is located at a distance of about 2.5 cm from the outlet and moves away forward. The surface of the horn is slightly furrowed.

Another find probably belongs to the same taxon of deer, an incomplete weakly worn upper tooth M3 (collection of NAS RA, IGN no. 10220/4119). The tooth has a low crown with wrinkled enamel (see Figs. 8b, 8c). At the base the crown is quite swollen. There is an additional column (entostyle); its height is ~1/3 of the crown height.

The characteristics of the horn allow us to attribute the deer find from the Noratus to representatives of the genus *Arvernoceros*. Deer of this genus were common in Europe in the Pliocene and early Pleistocene, starting from the end of the Ruscinium throughout almost the entire Villafranchian [1, 4, 5, 17–19, 22]. The base of the horn and the level of origin of the first process indicate a definite similarity with those of representatives of the genus from the Early Pleistocene of the Sea of Azov and Moldova (Fig. 9). Later, *Arvernoceros*

Fig. 7. Intralayer deformations (seismites), Noratus-2, sedimentary layer 6'.

possessed relatively more massive horns compared to the late Pliocene (early Villafranchian).

DISCUSSION OF THE RESULTS

Results of the Stratigraphic Studies

In the Noratus-1 outcrop, the lower 5 m are characterized by reverse magnetization, while the overlying 50 m are characterized by direct magnetization. Considering that the K–Ar age of the upper pumice layer in layer 1 is 2.3 ± 0.15 Ma, the underlying normally magnetized part of the section belongs to the Gauss paleomagnetic chron, while the reverse magnetized lower part of the section can correspond to the Caena subchron (3.032–3.116 Ma). Our analysis of the obtained spore-pollen data for the lower part of the section confirms this assessment (see Fig. 6). Thus, the age of the Noratus-1 deposits belongs to the

Table 1. The measurements of a paleontological find, that is, the horn of an extinct deer of the genus *Arvernoceros* sp. found in the Noratus-2 section

No.	Measured parameter	mm
1	Rosette diameter, lateromedial	57.5*
2	Rosette diameter, anteroposterior	63.6
	Rosette circumference	193*
	Angle of the first branch, deg	104
	Height of origin of the first process (length from the rosette to the distal surface of the base of the dorsal process)	75
3	Diameter of the base of the horn above the rosette, lateromedial	48*
4	Diameter of the base of the horn above the rosette, anteroposterior	63.2
	Circumference of the base of the horn	160*
5	Diameter of the base of the first process, lateromedial	39.5
6	Diameter of the base of the first process, anteroposterior	40.3
	Circumference of the base of the first process	135*
7	Rod diameter above the first process, lateral-medial	40.4
8	Rod diameter above the first process, anteroposterior	33.9
9	Index of flattening of the base of the horn (3/4)-?	0.76
10	Flattening index of the first process (5/6)-?	0.98
11	Rod flattening index (7/8) ?	1.19

*, restored parameters.

Fig. 8. Paleontological finds in section Noratus-2 in sedimentary layer 3'. (a), the horn of an extinct deer of the genus *Arvernoceros*; (b)–(c) deer tooth.

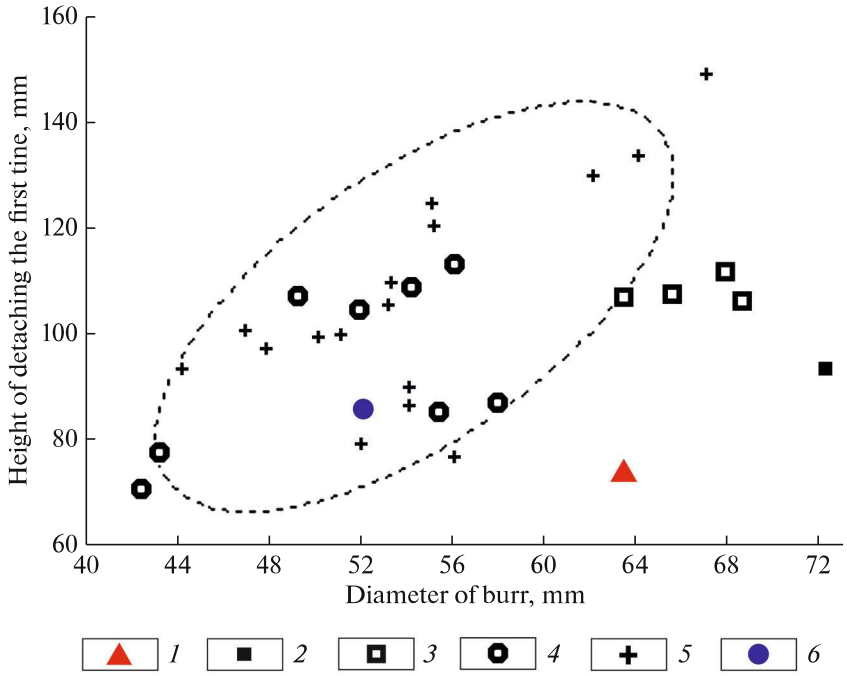

Fig. 9. Parameters of the base of the deer antler of the genus *Arvernoceros*. (*1*)–(*4*), A. verestschagini, Early Pleistocene: (*1*) Noratus-2; (*2*) Salchia; Liventsovka: (*3*) add; (*4*) subadd.; (*5*)–(*6*), A. ardei, Late Pliocene: (*5*) Atuer; (*6*) Kushkun.

~2.3–3.1 Ma interval and is older, which refines the primary age estimate of the studied deposits [8, 9].

The biostratigraphic data we obtained from the paleontological find of the antler of an extinct deer of the genus *Arvernoceros* sp. found in the Noratus-2 outcrop suggest that layer 3', which contains the bone remains, most likely belongs to the Akchagyl, i.e., Upper Pliocene or Gelasian. Since layers 3'–6' of the Noratus-2 section are normally magnetized, we attribute them to the Upper Pliocene and correlate them with layers 2–6 of Noratus-1. The gravel–pebble stratum occurring in the roof of the northwestern part of the Noratus-2 outcrop is nested and is of Pleistocene age.

Manychar lavas that overlie part of the Noratus-2 section and probably underlie the Noratus-1 section and whose analogs are dated at ~2.5 Ma [8, 9]; we consider them as effusives of a certain composition and appearance of different ages, but not a stratigraphic subdivision.

Upper Pliocene–Quaternary Noratus-1 and Noratus-2 deposits are exposed in the northern part of the Gavar horst near the plane of the Noratus fault, which limits the Gavar horst from the east. One of the branches of the Noratus fault with an amplitude of 10–15 m extends directly along the Noratus-1 outcrop (see Fig. 3a). The Noratus-2 deposits have a lower hypsometric position with a difference of several tens of meters compared to the Noratus-1 deposits, which is associated with a vertical displacement along the Noratus-Kanagekh zone as a whole.

The Artsvakar anticline is located within the Gavar horst. After the completion of the accumulation of Noratus-1 and Noratus-2 lake sediments, the runoff from the Geghama Highlands was carried out eastward to the Greater Sevan, as indicated by pebbles in the upper northwestern part of Noratus-2. The flow direction was also preserved after the Noratus-2 deposits were overlapped by the lavas of the Geghama Highlands. This is confirmed by the presence of drained valleys on the surface of lava flows, the largest of which are located in the southern parts of the Gavar horst.

As a result of the subsequent rise of the Gavar horst there was a change in the direction of the drainage from the Geghama highlands. The drainage began to be carried out to the north along the newly formed valley of the Gavaraget River with water discharge to the southwestern part of Lesser Sevan [13, 16]. The Gavar horst in the northern part is composed of sedimentary and volcanic-sedimentary deposits of Sevan, overlain by andesite-basalts and andesites Geghama highlands. Weakly lithified sedimentary thickness was covered with lavas, which preserved it from erosion. However, the northernmost part of the Gavar horst, located at the latitude of Noratus-1, due to having the greatest distance from volcanic centers, may not have been covered by lava flows, or the cover was thin and quickly eroded when the horst was uplifted. The maximum energy of flowing water from the redistributed runoff was concentrated in the area of the western flank of the Gavar horst, which contributed to its rapid erosion, while the eastern part of the horst has been preserved in the form erosion-tectonic remnant.

The Formation of the Sevan Intermountain Depression

To establish the time of the beginning of the formation of the Sevan intermountain depression, we relied on the following provisions, corresponding to the data we cited:

— in the Sarmatian, the Sevan region was part of the Ponto-Caspian basin and did not differ from it in an increased thickness of precipitation; the Sarmatian–Meotis boundary (~7.6 Ma) is a transition for the Sevan region from the maritime to the continental regime of development;

— in the Akchagylian time (from ~3.2 to 2.1 (1.8) Ma), the basin already sagged, which is confirmed by the Noratuz-1 section and the 86–117-meter lacustrine sandy-argillaceous strata in wells 2 and 4;

— in the interval between the Sarmatian and the Akchagyl (Meotis–Pont), no subsidence of the Sevan depression itself was recorded;

— Cimmerian alluvial-proluvial deposits with erosion occur on Sarmatian clays in well No. 4 (see Fig. 4);

— in the deposits of the Artsvakar anticline there is lacustrine malacofauna and thin layers of diatomites accumulated in small lakes of dammed genesis.

On the basis of the presented data, we believe that the depression occurred in the Pliocene–Quaternary time. Given the depth the position of the base of the Cimmerian deposits (Lower Pliocene) in wells 2 well 4, the minimum relative subsidence of the Sevan depression during this time ranged from ~550 to 650 m. In the central part of the depression, the subsidence could be more than 650 m.

To the west of the Sevan depression is another large intermountain depression of Armenia, the Shirak depression. The waters of the Akchagyl transgression of the Caspian penetrated into the Shirak depression, as evidenced by the discovery of marine Akchagyl deposits in its western part [30, 33].

There are no marine Akchagyl deposits in the Sevan depression; sedimentary strata of this age are represented by sandy-clayey deposits of a freshwater lake. It is most likely that the Sevan depression had a higher hypsometric position than the Shirak depression, i.e., had been involved in uplifting previously.

The thickness of the post-Akchagyl deposits in the south of the Greater Sevan depression (Masrik lowland) is ~300 m; in the central part of the depression the thickness can be greater. The maximum thickness of post-Akchagyl deposits in the Shirak depression is ~160 m [28]. This difference indicates that in the Qua-

ternary the Sevan depression experienced greater deflection compared to the Shirak depression.

The Genesis of the Sevan Intermountain Depression

The formation of the Sevan intermountain depression is associated with the development of fault zones that form the Sevan almond-shaped structure. Within the Sevan almond-shaped structure, similar structures of a smaller scale were identified, the pull-apart depression of the Lesser Sevan and the Geghama almond cavity. Thus, the basin morphology is determined by faults of various lengths and kinematics.

The Shirak basin located to the west is tectonomagmatic, i.e., its subsidence occurred as a result of deep geodynamic processes expressed by Pliocene–Quaternary volcanic activity [28].

The bottom bending of the Sevan depression occurred in a similar manner against the backdrop of volcanic activity in the Geghama and Vardenis highlands. This indicates that the bowing of the Sevan depression is associated not only with the regional stress field, as expressed by fault tectonics, but also with magmatism, i.e., the depression has a heterogeneous origin.

CONCLUSIONS

According to the results of the research, the authors came to the following conclusions:

(1) Sedimentary deposits of the Sevan depression have Middle Miocene–Quaternary age. Most of these deposits are lower along faults below the level of the day surface and only in the north of the western coast of Greater Sevan are brought to the day surface as part of the Gavar horst (including the explored Noratus-1 and Noratus-2 sections).

(2) The age of the Noratus-1 deposits was established on the basis of paleomagnetic data, isotope dating, and spore-pollen analysis as ~2.3–3.1 Ma, i.e., older than previously thought. The age of the deposits of the Noratus-2 outcrop was established on the basis of paleomagnetic data and a single find of fauna as the boundary of the Pliocene and Lower Pleistocene. These deposits are overlain by Lower Pleistocene large-pebble alluvium.

(3) The uplift of the Gavar horst was accompanied by erosion of its northwestern part due to the redistribution of the runoff from the Gegham highlands. The northeastern part of the horst with the Noratus-1 outcrop, bounded by the Noratus fault, has been preserved as an erosion remnant.

(4) In the Middle and Late Sarmatian, the region of the Sevan depression was part of the sea basin of the Eastern Paratethys. The subsidence of an already isolated depression can be considered established in the Pliocene–Quaternary time. The subsidence value was 550–650 m.

(5) When comparing the two largest intermountain depressions of Armenia, Shirak, and Sevan, the following was established. The Akchagyl transgression of the Caspian Sea reached the area of the Shirak depression, as evidenced by the presence of marine Akchagyl deposits on its western side, but did not reach the area of the Sevan depression, where lacustrine deposits accumulated in the Akchagyl time. Perhaps this is due to the tectonic isolation and higher hypsometric position of the Sevan depression in the Akchagyl time. The thickness of the post-Akchagyl deposits in the Sevan depression is approximately two times higher than in the Shirak depression, which indicates a more intense relative subsidence in the Quaternary.

(6) The Sevan intermountain basin probably has a heterogeneous genesis, due both to the impact of regional faults, primarily strike-slip tectonics, and deep-seated transformations, as expressed by Pliocene–Quaternary volcanism.

ACKNOWLEDGMENTS

The authors are grateful to N. Orlov (GIN RAS, Moscow, Russia) for restoration of the *Arvernoceros* sp. faunal find. The authors are grateful to anonymous reviewers for helpful comments and to the editor for careful editing.

FUNDING

This publication was prepared as part of the implementation of the RSF grant 22-17-00249 (Tesakov A.S.). Restoration and *Arvernoceros* sp. deer antler diagnostics has been carried out within the framework of the implementation of the state task of the SSC RAS, no. gr. Project 122011900166-9 (Titov V.V.). Field work supported Science Committee of the Ministry of Education, Science, Culture and Sports of the Republic of Armenia in the framework of the scientific project No. 15T-1E041.

COMPLIANCE WITH ETHICAL STANDARDS

Conflict of interests. The authors declare that they have no conflicts of interest.

REFERENCES

1. L. I Alekseeva, "Early Anthropogene theriofauna of Eastern Europe," in *Transactions of Geological Institute of Russian Academy of Sciences.* Vol. 300, Ed. by V. I. Gromov (Nauka, Moscow, 1977) [in Russian].
2. E. V. Arutyunyan, V. A. Lebedev, I. V. Chernyshev, and A. K. Sagatelyan, "Geochronology of Neogene–Quaternary volcanism of the Geghama Highland (Lesser Caucasus, Armenia)," Dokl. Earth Sci. **416**, 1042–1046 (2007)
3. G. P. Bagdasaryan and R. Kh. Gukasyan, *The Geochronology of Igneous, Metamorphic, and Ore Formations in*

Armenia (Akad. Nauk ArmSSR, Erevan, 1985) [in Russian].

4. I. A. Vislobokova, "Fossil deer of Eurasia," in *Transactions of Paleontological Institute of the USSR Academy of Sciences.* Vol. 240, Ed. by L. D. Tatarinov (Nauka, Moscow, 1990) [in Russian].
5. I. A. Vislobokova, V. V. Titov, A. V. Lavrov, D. B. Startsev, K. K. Tarasenko, and A. V. Lopatin, "Occurrence of the giant deer of the genus *Arvernoceros* in Taurida Cave, Crimea," Dokl. Biol. Sci. **487** (1), 115–118 (2019).
6. R. T. Dzhrbashyan, *Paleogene Volcanic Belts in the Closure Zone of the Tethys Ocean (Lesser Caucasus). Doctoral (Geol.-Mineral.) Dissertation* (KIMS, Tbilisi, 1990).
7. A. L. Knipper, "Oceanic crust in the Alpine fold belt composition (south Europe, western Asia, and Cuba)," in *Transactions of Geological Institute of Russian Academy of Sciences.* Vol. 267, Ed. by A. V. Peyve (Nauka, Moscow, 1975) [in Russian].
8. E. E. Milanovsky, "New data on the succession of Neogene and Quaternary sediments in Lake Sevan," Izv. Akad. Nauk SSSR. Ser. Geol., No. 4, 110–118 (1952).
9. Yu. V. Sayadyan, *Recent Geological History of Armenia* (Gitutyun, Erevan, 2009) [in Russian].
10. S. D. Sokolov, "Olistostromes and ophiolite nappes of the Lesser Caucasus," in *Transactions of Geological Institute of Russian Academy of Sciences.* Vol. 296 (Nauka, Moscow, 1977).
11. V. G. Trifonov and A. S. Karakhanyan, "Geodynamics and history of civilizations," in *Transactions of Geological Institute of Russian Academy of Sciences.* Vol. 585 (Nauka, Moscow, 2004).
12. E. Kh. Kharazyan, *Geology and Quaternary Volcanism of Armenia*, Ed. by O. A. Sarkisyan (GEOID, Yerevan, 2012) [in Russian].
13. A. Avagyan, *Estimation of the Sip Rates and the Recurrence Intervals of Strong Earthquakes on the Fault System of Pambak–Sevan–Sunik (Armenia): Segmentation and Relation with Volcanic Activity. PhD Thesis* (Montpellier II Univ., Montpellier, France, 2001).
14. A. V. Avagyan, "Active faulting and related seismic hazard in the Vanadzor depression area," Proc. NAS Rep. Armenia. Earth Sci. **62**, 48–57 (2009).
15. A. Avagyan, M. Sosson, A. Karakhanian, H. Philip, S. Rebai, Y. Rolland, R. Melkonyan, and V. Davtyan, "Recent tectonic stress evolution in the Lesser Caucasus and adjacent regions," Spec. Publ.—Geol. Soc. London **340**, 393–408 (2010)
16. A. Avagyan, L. Sahakyan, Kh. Meliksetian, A. Karakhanyan, V. Lavrushin, T. Atalyan, H. Hovakimyan, S. Avagyan, P. Tozalakyan, E. Shalaeva, Ch. Chatainger, S. Sokolov, A. Sahakov, and G. Alaverdyan, "New evidences of Holocene tectonic and volcanic activity of the western part of Lake Sevan (Armenia)," Geol. Quart. **64** (2), 288–303 (2020).
17. V. Baigusheva and V. Titov, "Large deer from the Villafranchian of Eastern Europe (Sea of Azov Region): Evolution and paleoecology," Quat. Int. **284**, 110–122 (2013).
18. R. Croitor, "Large-sized deer from the Early Pleistocene of Southeast Europe," Acta Palaeontol. Romaniae **4**, 97–104 (2005).
19. R. Croitor, *Plio–Pleistocene Deer of Western Palearctic: Taxonomy, Systematics, Phylogeny*, Ed. by I. Toderaş (Elan Poligraf Publ., Chişinău: Moldova, 2018).
20. V. Davtyan, E. Foerflinger, A. Karakhanyan, H. Philip, A. Avagyan, C. Champollion, and R. Aslanyan, "Fault slip rates in Armenia by the GPS Data," Proc. Nation. Acad. Sci. Armenia. Ser.: Earth Sci. **59** (2), 3–18 (2006).
21. M. Hässig, Y. Rolland, M. Sosson, Gh. Galoyan, L. Sahakyan, G. Topuz, Ö. F. Çelik, A. Avagyan, and C. Müller, "Linking the NE Anatolian and Lesser Caucasus ophiolites: Evidence for large-scale obduction of oceanic crust and implications for the formation of the Lesser Caucasus-Pontides Arc," Geodinam. Acta **26** (3–4), 311–330 (2013).
22. E. Heintz, "Les cervides Villafranchiens de France et d'Espagne," Mem. Mus. Hist. Nat., C **22** (1), (1970).
23. A. Karakhanian, R. Djrbashian, V. Trifonov, H. Philip, S. Arakelian, and A. Avagian, "Holocene-historical volcanism and active faults as natural risk factor for Armenia and adjacent countries," J. Volcanol. Geotherm. Res. **113** (1–2), 319–344 (2002).
24. A. S. Karakhanian, V. G. Trifonov, H. Philip, S. Arakelian, and A. Avagyan, "Active faulting and natural hazards in Armenia, the Eastern Turkey and the Northwestern Iran," Tectonophysics **380**, 189–220 (2004).
25. A. Karakhanyan, A. Arakelyan, A. Avagyan, H. Baghdasaryan, R. Durgaryan, and Ye. Abgaryan, *The Seismotectonic Model, Seismic Hazard Assessment for the Construction Site of a New Power Unit of the Armenian NPP* (Yerevan: Ministry of Energy of the Republic of Armenia, Vienna, 2011. "NorAtom" Consortium Final Rep.).
26. H. Philip, A. Avagyan, A. Karakhanian, J.-F. Ritz, and S. Rebai, "Slip rates and recurrence intervals of strong earthquakes along the Pambak–Sevan–Sunik fault (Armenia)," Tectonophysics **343**, 205–232 (2001).
27. Y. Rolland, G. Galoyan, M. Sosson, R. Melkonyan, and A. Avagyan, "The Armenian ophiolite: Insights for Jurassic back-arc formation, Lower Cretaceous hot spot magmatism and Upper Cretaceous obduction over the South Armenian block," Spec. Publ.—Geol. Soc. London **340**, 353–382 (2010).
28. L. Sahakyan, D. Bosch, M. Sosson, A. Avagyan, Gh. Galoyan, Y. Rolland, O. Bruguier, Zh. Stepanyan, B. Galland, and S. Vardanyan, "Geochemistry of the Eocene magmatic rocks from the Lesser Caucasus area (Armenia): Evidence of a subduction geodynamic environment. Tectonic Evolution of the Eastern Black Sea and Caucasus," Spec. Publ.—Geol. Soc. London **428**, 73–98 (2017).
29. E. A. Shalaeva, V. G. Trivonov, V. A. Lebedev, A. N. Simakova, A. V. Avagyan, L. H. Sahakyan, D. G. Arakelyan, S. A. Sokolov, D. M. Bachmanov, A. A. Kolesnichenko, A. V. Latyshev, E. V. Belyaeva, V. P. Lyubin, P. D. Frolov, A. S. Tesakov, E. K. Sy-

chevskaya, G. V. Kovalyova, M. Martirosyan, and A. I. Khisamutdinova, "Quaternary geology and origin of the Shirak Basin, NW Armenia," Quat. Int. **509**, 41–61 (2019).

30. A. N. Simakova, A. S. Tesakov, H. Celik, P. D. Frolov, E. A. Shalaeva, S. A. Sokolov, Ya. I. Trikhunkov, V. G. Trifonov, D. M. Bachmanov, A. V. Latyshev, P. B. Ranjan, O. V. Gaydlenok, E. V. Syromyatnikova, G. V. Kovaleva, and M. A. Vasilieva, "Caspian-type dinocysts in NE Turkey mark deep inland invasion of the Akchagylian brackish-water basin during the terminal Late Pliocene," Quat. Int. **605–606**, 329–348 (2021).
31. M. Sosson, Y. Rolland, C. Müller, T. Danelian, R. Melkonyan, S. Kekelia, S. Adamia, V. Babazadeh, T. Kangarli, A. Avagyan, G. Galoyan, J. Mosar, "Subductions, obduction and collision in the Lesser Caucasus (Armenia, Azerbaijan, Georgia): New insights," Spec. Publ.—Geol. Soc. London **340**, 329–352 (2010).
32. V. G. Trifonov, A. S. Karakhanian, and A. I. Kozhurin, "Major active faults of the collision area between the Arabian and the Eurasian plates," in *Proceedings of International Conference "Continental Collision Zone Earthquakes and Seismic Hazard Reduction"* (IASPEI/IDNDR Publ., Yerevan, Armenia, 1994), pp. 56–78.
33. A. S. Tesakov, E. A. Shalaeva, P. D. Frolov, Ya. I. Trikhunkov, E. A. Zelenin, G. N. Aleksandrova, D. M. Bachmanov, A. V. Latyshev, D. V. Ozherelyev, S. A. Sokolov, and E. V. Belyaeva, "The Upper Pliocene–Quaternary geological history of the Shirak basin (NE Turkey and NW Armenia) and estimation of the Quaternary uplift of Lesser Caucasus," Quat. Int. **546**, 229–244 (2020).